Dynamic-Statistic Combined Ensemble Prediction and Impact Factors on China's Summer Precipitation

Xiaojuan Wang[1], Zihan Yang[2*], Shuai Li[3], Qingquan Li[3], Guolin Feng[3, 4*]

1 College of Electronic and Information Engineering, Changshu Institute of Technology, Suzhou, 215506, China

2 Department of Atmospheric Sciences, Yunnan University, Kunming, 650500, China

3 Laboratory for Climate Research, National Climate Center, Beijing, 100081, China

4 College of Physical Science and Technology, Yangzhou University, Yangzhou, 225009, China

Abstract The dynamic-statistic prediction shown excellent performance on monthly and seasonal precipitation prediction in China and has been applied on several dynamical models. In order to further improve the prediction skill of summer precipitation in China, the Unequal-Weighted Ensemble prediction (UWE) using outputs of the dynamic-statistic prediction is presented, and its possible impact factors are also analyzed. Results indicate that the UWE has shown promise in improving the prediction skill of summer precipitation in China, on account to the UWE can overcome shortcomings of the structural inadequacy of individual dynamic-statistic prediction, reducing formulation uncertainties, resulting in more stable and accurate predictions. Impact factors analysis indicates that 1) the station-based ensemble prediction with ACC being 0.10-0.11 and PS score being 69.3-70.2, has shown better skills than the grid-based one, as the former produces probability density distribution of precipitation being closer to the observation than the latter. 2) The use of the spatial average removed anomaly correlation coefficient (SACC) may lower the prediction skill and introduce obvious errors on estimating the spatial consistency of prediction anomalies. SACC could be replaced by the revised anomaly correlation coefficient (RACC), which is calculated directly using the precipitation anomalies of each station without subtracting the average precipitation anomaly of all stations. 3) The low dispersal intensity among ensemble samples of UME implies the historical similar error selected by different approach is quite close to each other, making the correction on the model prediction is more reliable. Therefore, the UWE is expected to further improve the accuracy of summer precipitation prediction in China by considering impact factors such as the grid

Zihan Yang
2622261772@qq.com
Guolin Feng
fenggl@cma.gov.cn

32 or station-based ensemble approach, the method of calculating the ACC, and the

33 dispersal intensity of ensemble samples in the application and analysis process of UWE.

34

35 **Keywords**: Dynamic-statistic prediction, Unequal weighted ensemble prediction,

36 Prediction accuracy, Dispersal intensity, Revised anomaly correlation coefficient

37

38

Introduction

Accurate prediction of summer precipitation across China is paramount for dealing with critical issues such as flood and drought management, economic development, and ensuring food security. However, this task is fraught with challenges due to the intricate interplay among various atmospheric circulation components, including the East Asian summer monsoon (Ding 1994, Lu 2005), the Northwest Pacific subtropical high (Tao 2006), and the East Asia-Pacific teleconnection patterns (Huang 1987, Huang 2004). Additionally, external influences, such as the El Niño-Southern Oscillation (ENSO) (Sun, Yang et al. 2021) and the snow cover on the Tibetan Plateau (Si and Ding 2013), further complicate the prediction process. Some studies have also shown that improving the Real-time Multivariate Madden-Julian Oscillation (RMM) index or introducing better intraseasonal signal extraction methods may allow for higher predictability limits in real-time forecasting (Ding and Seo 2010). Due to these complexities, increasing the accuracy of summer rainfall prediction in China still faces challenges, the pursuit of more precise summer rainfall predictions in China is an endeavor that warrants the utmost attention from climate scientists (Wang, Schepen et al. 2012, Gong, Hutin et al. 2016).

Over the past few decades, there has been a remarkable progression in the foundation of observational data and theoretical understanding, which has significantly enhanced the capabilities of climate dynamical models in predicting seasonal rainfall (Wu, Vitart et al. 2017, Gettelman, Geer et al. 2022). High-resolution climate simulations, such as those with atmospheric resolutions of approximately 50 km and oceanic resolutions of 0.25°, have been successfully implemented by several research institutions (Satoh, Tomita et al. 2014, Roberts, Hewitt et al. 2016, Wu, Yu et al. 2021). These dynamic models have also demonstrated success in long-term prediction of atmospheric circulation patterns and sea surface temperatures in low-latitude regions (Zhu and Shukla 2013). However, the current performance of seasonal predictions for key climate elements, including rainfall and temperature, particularly in monsoon-influenced areas like East Asia (Wang, Fan et al. 2015, Gong, Dogar et al. 2017), remains somewhat constrained due to inherent limitations in parameterization schemes and the challenges associated with boundary value problems (Wang, Fan et al. 2015). This has spurred meteorologists to delve deeper into understanding how to effectively enhance the seasonal prediction skills of climate models to better align with the needs of end-users (Gong, Hutin et al. 2016). It is well recognized that regional climate

73 characteristics can significantly influence local rainfall patterns, atmospheric

74 predictability varies significantly between regions, altitudes and seasons (Li and Ding

75 2011). Despite this, dynamic models still struggle to accurately capture these nuances,

76 suggesting that there is potential for improvement in rainfall prediction through a

77 statistical-dynamic approach (Specq and Batté 2020). This integrated methodology

78 could provide a more robust framework for prediction, ultimately leading to more

79 reliable and actionable climate predictions. The relative impact of initial condition and

80 model uncertainties on local predictability also varies with the system state. Therefore,

81 strategically reducing uncertainties in sensitive regions can effectively improve

82 forecasting skills (Li, Ding et al. 2020). Apart from that, warm events are easier to

83 predict than cold events (Li, Ding et al. 2020).

84   To enhance the precision of rainfall prediction, Chou (1974) initially suggested

85 the integration of dynamical model data with statistical analogue information. This

86 approach leverages the prediction errors from historical years with analogous initial

87 conditions, such as similar circulation anomalies, snow cover, and sea surface

88 temperatures (SST), to refine dynamic-analogue correction techniques. For instance,

89 Huang, Yi et al. (1993) introduced the evolutionary analogue-based multi-time

90 prediction method, (Ren and Chou 2006, Ren and Chou 2007) employs historical

91 analogue data to estimate model errors in accordance with the atmospheric analogy

92 principle, (Feng, Zhao et al. 2013, Feng, Yang et al. 2020) further develops this concept

93 with their correction method focused on key regional impact factors. Wang and Fan

94 (2009) proposed a scheme that integrates model forecasts with the observed spatial

95 patterns of historical "analog years," while Gong, M. et al. (2018) advanced the leading

96 mode-based correction method. In addition to these advancements, dynamic-statistic

97 correction methods have been successfully applied to rainfall predictions in regions

98 such as North China (Yang, Zhao et al. 2012) and Northeast China (Xiong, Feng et al.

99 2011). Furthermore, the application of these dynamic-statistic prediction has been

100 extended to seasonal predictions, including those for autumn, winter, and spring (Lang

101 and Wang 2010). At the Beijing Climate Center, various error selection methods have

102 been operationalized in rainfall prediction, including the raw field-based similar error

103 selection method, the empirical orthogonal function-based similar error selection

104 method, the grid-based similar error selection method, the regional key impact factors-

105 based similar error selection method, and the abnormal factor-based similar error

106 selection method (Feng, Yang et al. 2020). These innovative approaches underscore the

107 ongoing efforts to harness both dynamical and statistical insights to achieve more
108 accurate and reliable rainfall predictions.

109 Research has consistently demonstrated the benefits of integrating predictions
110 from multiple climate models. For instance, the Bayesian model averaging approach
111 (Luo, Wood et al. 2007) and the moving coefficient ensemble approach (Yang, Bai et
112 al. 2024) are two such approaches that have shown promise. The use of a multi-model
113 ensemble can mitigate the collective local biases that can occur in space, time, and
114 across different variables when using individual models (Krishnamurti, Kumar et al.
115 2016). This approach not only assigns higher weights to the outputs of more accurate
116 models but also enhances overall predictive skill and reduces the uncertainty associated
117 with single-model ensembles (Yan and Tang 2013). By accounting for comprehensive
118 uncertainties stemming from both model discrepancies and initial conditions, multi-
119 model ensembles often outperform single models (Palmer, Alessandri et al. 2004).
120 Furthermore, the diverse assumptions inherent in different model frameworks can
121 potentially compensate for our incomplete understanding of atmospheric dynamics
122 (Yan and Tang 2013). The multi-model approach has been successfully applied across
123 a broad spectrum of forecasting needs, including medium-range weather forecasting
124 (Candille 2009) and seasonal climate prediction (Vitart 2006). Given the
125 aforementioned advantages of dynamic-statistic methods in seasonal predictions, it is
126 imperative to adopt an ensemble approach that combines the predictions from these
127 methods. This integration is crucial for further enhancing prediction accuracy and
128 reliability. By leveraging the collective strengths of various models and techniques, we
129 can achieve a more robust and nuanced understanding of climate patterns, ultimately
130 leading to improved prediction capabilities.

131 In the process of examining the ensemble prediction, it is crucial to take into
132 account the various factors that can influence its predictive accuracy (Krishnamurti and
133 Kumar 2012). The ensemble's output is particularly sensitive to several key elements:
134 the number of models incorporated, the duration of the dataset utilized for training, and
135 the distribution of weights for both downscaling and the integration of multiple models
136 or schemes (Krishnamurti, Kumar et al. 2016). Both grid-based reanalysis data and
137 station-based observational data can serve as the foundation for model training or
138 validation (Ding, Li et al. 2004, Wang, Fan et al. 2015, Gong, Hutin et al. 2016). It is
139 therefore essential to explore and discuss the differential impact that the use of these
140 two distinct types of datasets may have on ensemble predictions. Furthermore, the

dispersion of samples across different models or methodologies cannot be overlooked, as it also affects the ensemble's predictive skill, and deserve certain attention (Houze, Rasmussen et al. 2015).

Based on above statement, the aim of this research is to construct an Unequal-Weighted Ensemble prediction (UWE) employing a comprehensive array of dynamic-statistic methods and to explore the potential factors that may influence its predictive capabilities. Specifically, the study is designed to delve into three primary areas: (1) Elucidate the process of establishing the UWE through a suite of dynamic-statistic methods, highlighting the distinctions between grid-based ensembles and station-based ensembles. (2) Examine the most effective methodologies for evaluating the spatial congruence between observational data and the UWE's output. (3) Investigate the connection between the dispersal of samples across various dynamic-statistic methods and the predictive accuracy of the UWE. This study will provide a comprehensive analysis of the UWE's development and its performance, offering valuable insights into the factors that influence its predictive success.

1 Data and Method

1.1 Data

The monthly precipitation data of 1634 stations during 1983–2020 are from the National Meteorological Information Center of the China Meteorological Administration. The monthly grid precipitation data during 1983–2020 is derived from the Combined Rainfall Analysis (CMAP) data of the U.S. Climate Prediction Center. The model prediction data for summer precipitation in China are hindcast datasets of the BCC_CPSv3. Monthly climate indices during 1983–2020 including circulation indices (i.e. AO, AAO), SST indices (i.e. Nino 3.4, Nino 4, Pacific Decadal Oscillation), snow cover indices (i.e. Tibet snow cover area index, Northeast China snow cover area index) is available from the Beijing Climate Center website (http://cmdp.ncc-cma.net/Monitoring/ cn_index_130.php) (Gong, Hutin et al. 2016).

1.2 Climate regions division

Climate in China influence by various climate systems, such as the Monsoon, mid-high latitude circulation system and westly jet circulation system, etc. (Ding 1994, Li, Dai et al. 2008, Wu, Vitart et al. 2017). Since summer rainfall has regional characteristics and potential impact factors, we divide the whole country into 8 regions (Feng, Yang et al. 2020) in terms of South China (110º~120ºE, 20º~25ºN), East China

(110º~123ºE, 25º~35ºN), North China (110º~123ºE, 35º~42.5ºN), Northeast China (110º~135ºE, 42.5º~55ºN), Eastern Northwest China (90º~110ºE, 35º~43ºN), Western Northwest China (75º~90ºE, 35º~48ºN), Tibet Area (80º~100ºE, 27º~35ºN and Southwest China (95º~110ºE, 22º~33ºN). Each region is treated separately by the dynamic-statistic prediction process.

1.3 The dynamic-statistic predictions

Numerical model is an approximation of the behavior of the actual atmosphere. The dynamic-statistic prediction is to utilize the information of historical analogues to estimate model's prediction errors through the statistical method, thereby to compensate the model deficiencies and reduce the model errors (Huang, Yi et al. 1993). As addressed by Feng, Yang et al. (2020), the dynamic-statistic prediction can be explained by equation (1),

$$\hat{p}(\psi_0) = p(\psi_0) + \tilde{p}(\psi_j) - p(\psi_j), \qquad (1)$$

Where $\hat{p}(\psi_0)$ is the corrected prediction, $p(\psi_0)$ is the original model prediction, and $p(\psi_j)$ is the model prediction of historical year having the similar initial conditions as current one, $\tilde{p}(\psi_j)$ is the corresponding historical observation. Eq. (1) is the integral form of the similarity error correction equation, in which the error term of the similar historical prediction $\tilde{p}(\psi_j) - p(\psi_j)$ is added to the prediction results of the numerical model.

$$\hat{p}(\psi_0) \xrightarrow{Estimate} \hat{E}(\psi_0), \qquad (2)$$

The core idea of the dynamic-statistic prediction is developing the scheme how to select the similar year and estimate historical prediction errors(Feng, Zhao et al. 2013, Gong, Hutin et al. 2016). Eq. (2) transforms improvement in the dynamical model prediction into the estimation of model error (Ren and Chou 2006, Xiong, Feng et al. 2011, Feng, Zhao et al. 2013).

1.4 Schemes for the dynamic-statistic prediction

Fig.1 presents the flow chart of the dynamic-statistic prediction method. The key step is the scheme for selecting the historical similar years, which is the step in the red box. Different scheme of selecting similar years from the historical dataset corresponds to different dynamic-statistic prediction scheme. In previous years, a series of the dynamic-statistic prediction schemes has been developed for selecting similar years from the historical information, and excellent results have been achieved in predicting

207 summer precipitation anomalies in China (Wang and Fan 2009, Xiong, Feng et al. 2011,

208 Feng, Zhao et al. 2013, Wang, Fan et al. 2015).

209
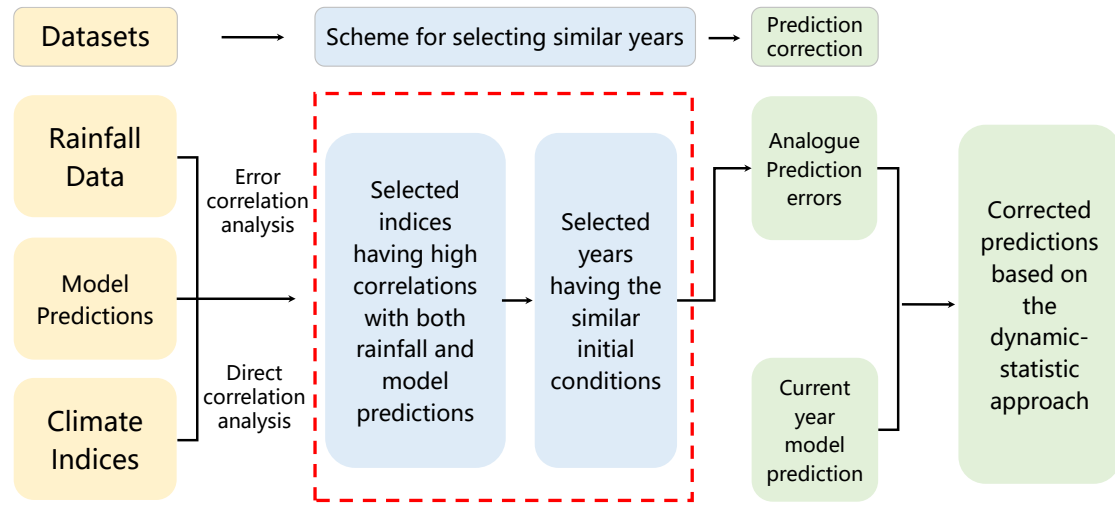
211 **Fig. 1** The flow chart of the dynamic-statistic prediction method. The key step is the

212 scheme for selecting the historical similar years, which is the step presented in the red

213 dash box. The climate indices refer to the 130 monthly climate indices in terms of the

214 SST indices, Circulation indices etc. during 1983－2020 in section 1.1

215

216 Five kinds of the dynamic-statistic prediction approach representing different

217 scheme for analogue error selection are introduced as follows,

218 1) The scheme for original model prediction-based similar error selection (ORM).

219 With the dynamical model original prediction, select four historical years has the most

220 similar feature of anomaly distribution as the current year's prediction. Then calculate

221 the analogue prediction error using these similar years, add to the current prediction

222 and produce the corrected prediction.

223 2) The scheme for Empirical Orthogonal Function mode-based similar error

224 selection (EOF). Calculating the model prediction error filed and produce the

225 corresponding spatial modes and corresponding principal components using the EOF

226 method. Similar years is selected based on the Euclidean distance of the principal

227 components. Historical similar error is calculated using the selected similar years and

228 added to the current model prediction, which then produce the corrected prediction

229 (Gong, M. et al. 2018).

230 3) The scheme for the regional average precipitation-based similar error selection

231 (REG). Dividing the whole country into 8 regions using according to the introduction

of section 1.2. Selecting the climate indices having high correlations with the regional average precipitation of each region. With these highly correlated indices, multi-factors are randomly configured and used to calculate the shortest Euclidean distance to choose the historical similar years and produce the similar error. Cross-validation are carried out to correct the model prediction error and obtain the optimal multi-factor configuration. Based on this final optimal multi-predictor configuration, the dynamic-statistic prediction can be implemented (Xiong, Feng et al. 2011).

4) The scheme for the grid precipitation-based similar error selection (GRD). The similar error selection is the same as the REG approach, but the model prediction error correction is carried out on each grid point within a region.

5) The scheme for the abnormal factors based similar error selection (ABN). Establish factors having significant correlations with the regional precipitation. Determine the anomaly threshold of each factor and select the key factors reaching the threshold. Based on the selected abnormal factors, similar years are selected by the shortest Euclidean Distance of factor set between current year and historical years. Then the analogue errors can be calculated by using the method of weighted average integration and be added on the current year's model prediction, which can produce the corrected prediction (Feng, Yang et al. 2020).

6) The scheme for systematic error selection (SYS). The arithmetic mean of the model prediction errors over the years is calculated, after which it is superimposed on the model's original prediction results to obtain the systematic error revised prediction of the systematic error revised prediction of the model. This scheme is primarily used for comparison with the other five dynamic-statistic schemes.

The selected similar years are not consistent with each other among these five schemes, the analogue errors usually show similar pattern, but have difference in detail. Besides the dynamic-statistic prediction, the system error correction are also presented for comparison.

1.5 The Dynamic-Statistic Combined Ensemble Prediction

In order to further improve the effectiveness of summer precipitation prediction by various dynamic-statistic schemes, this study conducted the Dynamic-Statistic Combined Ensemble Prediction called Unequal-Weighted Ensemble prediction (UWE).

Based on the five the dynamic-statistic prediction schemes, the unequal

265 weighting ensemble prediction (UWE) E_m is calculated as equation (3),

$$E_m = \sum_{k=1}^{n} w_{km} F_{km} \quad (n=5)$$, (3)

267 Where F_{km} is the single prediction of each dynamic-statistic scheme and w_{km} is

268 the weight coefficient of each member. n denotes the total number of dynamic-

269 statistic scheme, m denotes the current prediction year. w_{km} can be calculated

270 using equation (4). Using a method similar to the cross check, the TCC was calculated

271 by removing the precipitation predictions of the screened members along with the

272 precipitation actuals for the m th ($m \in [1,10]$) year of data.

$$w_{km} = \frac{T_{km}}{\sum_{k=1}^{n} |T_{km}|}$$ (4)

274 The weights w_{km} were calculated for each member at each grid-point in the year m ,

275 where T_{km} is the TCC value calculated for the knd member at that station or grid

276 point after excluding the precipitation data in year m , and $w_{km}(k=1,2,...,n)$ is the

277 weight of the krd member at that grid-point in year m . The anomaly correlation

278 coefficient (ACC), PS score, and root mean standard error are used for evaluating the

279 prediction skill for summer precipitation in China. The PS score can be calculated

280 using equation (5).

$$PS = \frac{f_0 \times N_0 + f_1 \times N_1 + f_2 \times N_2}{N - N_0 + f_0 \times N_0 + f_1 \times N_1 + f_2 \times N_2 + M} \times 100 ,$$ (5)

282 Where N is the total number of stations, is the number of the correctly predicted

283 stations with abnormal within (-20%, 20%), f_0 is weight coefficient of N_0 ; N_1 and

284 f_1 are for the stations with abnormal within (-50%, -20%) or (20%, 50%); N_2 , f_2

285 are for the stations with abnormal within (-100%, -50%) or (50%, 100%); M is the

286 total number of correctly predicted stations with abnormal below -100% or above 100%.

287 In this study, we set $f_0 = 2$, $f_1 = 2$ and $f_2 = 4$.

288 Normally, the spatial average removed ACC (SACC) is calculated by formular (6)

289 to assess the spatial consistency of prediction for summer precipitation in China (Xiong,

290 Feng et al. 2011, Fan, Liu et al. 2012).

$$291 \qquad R = \frac{\sum_{i=1}^{n}(x_i - \overline{x}_s)(y_i - \overline{y}_s)}{\sqrt{\sum_{i=1}^{n}(x_i - \overline{x}_s)^2 \sum_{i=1}^{n}(y_i - \overline{y}_s)^2}} \,, \qquad (6)$$

292 Where n is the total number of stations, x_i is the summer precipitation abnormal of

293 observation at station i, while y_i is the summer precipitation abnormal of prediction

294 at station i. $\overline{x}_s$ and $\overline{y}_s$ are respectively the average abnormal of observation and

295 prediction for all the stations. This so-called SACC need to subtract the average

296 precipitation anomaly of all stations from precipitation anomaly of each station before

297 calculating the ACC.

298   In order to confirm if the SACC can properly estimate the spatial consistency of

299 prediction for summer precipitation, we also calculated the revised anomaly correlation

300 coefficient (RACC) using formular (7),

$$301 \qquad R^* = \frac{\sum_{i=1}^{n}(x_i^o - \overline{x}_{i,t})(y_i^o - \overline{y}_{i,t})}{\sqrt{\sum_{i=1}^{n}(x_i^o - \overline{x}_{i,t})^2 \sum_{i=1}^{n}(y_i^o - \overline{y}_{i,t})^2}} \qquad (7)$$

302 Where n is the total number of stations, x_i^o and y_i^o are respectively the summer

303 precipitation of observation and prediction at station i. $\overline{x}_{i,t}$ and $\overline{y}_{i,t}$ is the average of

304 observation and prediction of summer precipitation for all the years at each station i.

305 The RACC is calculated directly using the precipitation anomalies of each station

306 without removing the average precipitation anomaly of all stations.

307 **2 The summer precipitation prediction using the dynamic-statistic scheme**

308   The RACCs and PSs of the summer precipitation in China produced by the five

309 dynamic-statistic methods are presented in Table 1. The 10-year average of PS score of

310 the dynamic-statistic methods varied from 67.4-69.6, which have the better

311 performance than that of the SYS method (65.8). In figure 2, the temporal correlation

312 coefficients of the dynamic-statistic methods are higher than the SYS method over most

313 China with the distribution spatial pattern is similar to each other, but the most improved

314 areas varied among different method. It is further confirmed with previous studies that

315 the merger of prediction error estimated via the statistical method and dynamic model-

316 based original output represents a potential means for improving prediction skill of

317 summer rainfall in China (Feng, Yang et al. 2020).

318

319 **Table 1** 10-year average of RACC and PS of the summer precipitation prediction

from 2011 to 2020 for the dynamic-statistic predictions and system error correction.

Scheme	ORM	EOF	REG
RACC	0.10	0.03	0.01
PS	69.5	69.6	67.4
Scheme	**GRD**	**ABN**	**SYS**
RACC	0.05	0.02	-0.08
PS	68.2	69.4	65.8
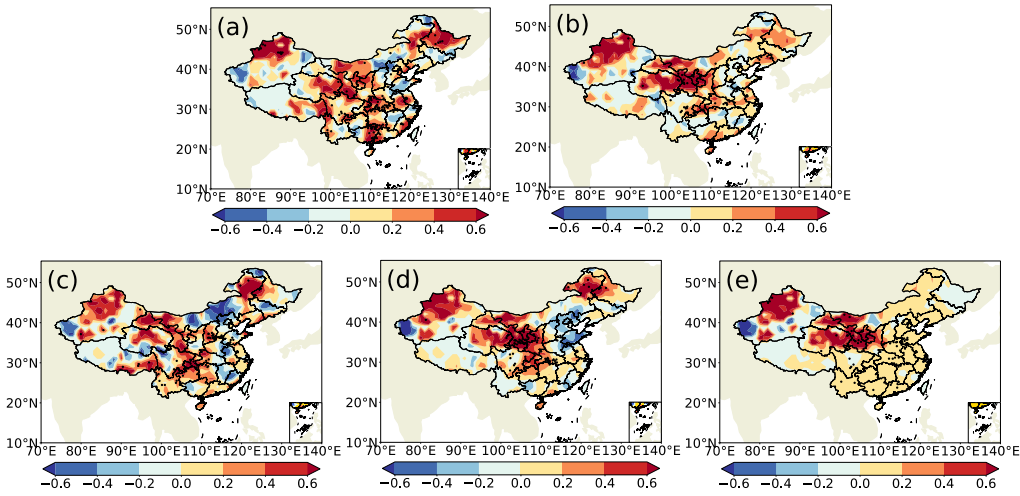
Fig. 2 The differences of the temporal correlation coefficients for summer precipitation predictions in China from 2011 to 2020. Values indicate differences of the dynamic-statistic method minus the SYS method. (a) ORM, (b) EOF, (c) REG, (d) GRD, and (e) ABN.

Based on the equation of formular (1), four schemes of UWE prediction using the single dynamic-statistic predictions as ensemble members and their corresponding one year out cross validations are presented in Table 2. In order to distinguish the performances UWE prediction against the grid-point observation and station observation, both the grid-based ensemble and station-based ensemble are calculated. Comparing with the single scheme of the dynamic-statistic prediction, the E4 scheme has the best skill among the four ensemble schemes, with RACC being 0.9 and PS score being 70. The grid-based ensemble can somewhat improve the summer precipitation prediction in China, but its effect varied among different schemes. The skills of the station-based ensemble are obviously better than the grid-based one, with RACC being 0.10-0.11 add PS score being 69.3-70.2. As addressed by Yan and Tang (2013) the

multi-model ensemble approach (MME) considers the structural inadequacy of individual models and can reduce model formulation uncertainties. The reason why the ensemble of multiple dynamic-statistic predictions can improve the summer precipitation in China is similar to that of MME, which can somewhat overcome the shortcomings of a single prediction and produce the more stable prediction.

Table 2 10-year average of RACC and PS score of summer precipitation prediction of the four UWE in China during 2011 ~ 2020.

Ensemble Scheme	Ensemble member	Grid Ensemble		Station Ensemble	
		RACC	PS	RACC	PS
E1	ORM, GRD	0.04	69.2	0.11	69.3
E2	ORM, GRD, EOF	0.07	69.3	0.11	70.2
E3	ORM, GRD, EOF, REG	0.08	69.9	0.11	70.7
E4	ORM,GRD,EOF,REG,ABN	0.09	70.0	0.10	70.1
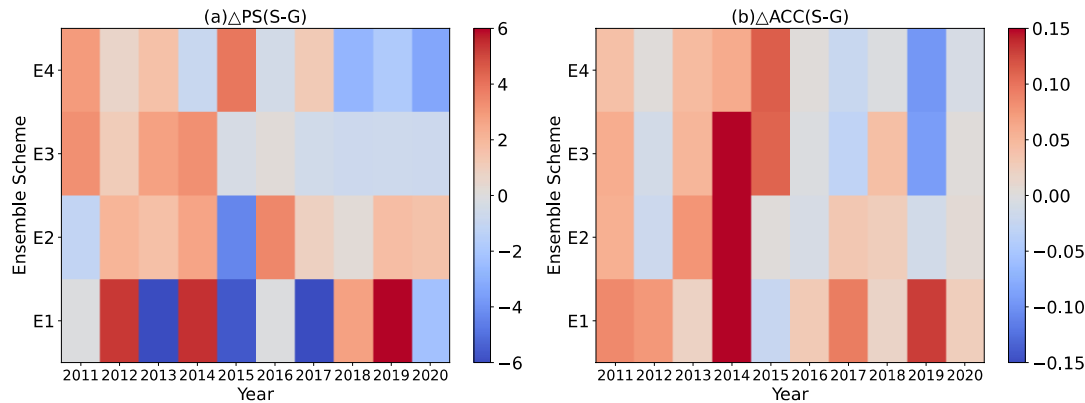
Fig. 3 Scatter distribution of differences of (a) PS and (b) RACC for summer precipitation prediction during 2011-2020 between station-based and grid-based UWE. Values indicate the differences of station-based ensemble minus the grid-based ensemble.

Figure 3 shows that there is no significant difference between the PS scores of the station-based and grid-based UWE for the E1 scheme. However, for the E2 scheme, the station-based UWE clearly outperforms the grid-based UWE. Additionally, the station-based UWE of E3 and E4 schemes also has relatively higher PS scores. RACC values, of the station-based prediction for all four schemes are generally higher than those for

360 the grid-based UWE. In summary, compared to the grid-based UWE, the station-based

361 one have obvious higher PS scores and RACC values, indicating better prediction

362 performance.

363 In Fig. 4, the TCC of the station-based ensemble for summer precipitation

364 prediction show positive values in most China, with the high value centers distributed

365 in western South China, central China, southern North China and western Northeast

366 China, etc. The similar spatial distributions are observed in predictions of the four

367 station-based ensemble schemes (Fig. 4 a, c, e, g). The TCC differences between the

368 station-based ensemble and the grid-based ensemble indicate that the former has higher

369 than values than the later in most areas of China, except for part of Central China and

370 East China (Fig. 4 b, d, f, h). The spatial distribution of TCC indicates the improvement

371 of the station-based ensemble is suitable for most stations in China and implies this

372 approach can make the summer precipitation prediction being closer to the observation.

373 Bueh, Shi et al. (2008) also addressed that the training phase of multi-model ensemble

374 learns from the recent past performances of models and is used to determine statistical

375 weights from a least square minimization via a simple multiple regression. During the

376 training process, more precise objective data can produce better weight coefficients and

377 lead to more accurate ensemble result, which might be the reason for the station-based

378 ensemble produce better predictions of summer precipitation in China than the grid-

379 based one.

380 Fig.5 indicates that the probability density distribution of station-based ensemble

381 predictions is closer to the observation especially at the peak part than the gird-based

382 ensemble and this feature is observed in four ensemble predictions. If the onsite

383 observation dataset can be used for training, we may have a parameterization scheme

384 containing precise information for each single station, which may be of help to produce

385 the prediction being close to the real situation of summer precipitation in China. Since

386 the gird-based dataset normally is the reproduced observation data, which may lose

387 certain precise information especially for those extreme values. This flaw of the grid

388 data may cause it to have poor performance on improving the prediction accuracy than

389 the station data(Xiong, Feng et al. 2011, Kim, Webster et al. 2012, Yang, Bai et al. 2024).

390 The station-based and grid-based UWE, as well as the actual precipitation data, all

391 exhibit characteristics of a normal distribution in Fig.5, instead of the typical skewed

392 distribution. This is primarily because this study focuses on summer precipitation over

393 the entire China region, which covers a large area and spans a long period rather than

394 the precipitation in a single grid or station in a short period. Within this range, various
395 types of precipitation events, including light, moderate, and heavy rain, make the
396 probability distribution closer to the normal distribution. Besides, In Fig. 5, probability
397 distribution is calculated based on the monthly anomaly precipitation, and after a
398 treatment of probability function of python program, which smooth the distribution
399 curve. Therefore, the final probability distribution appears as a normal distribution.

400
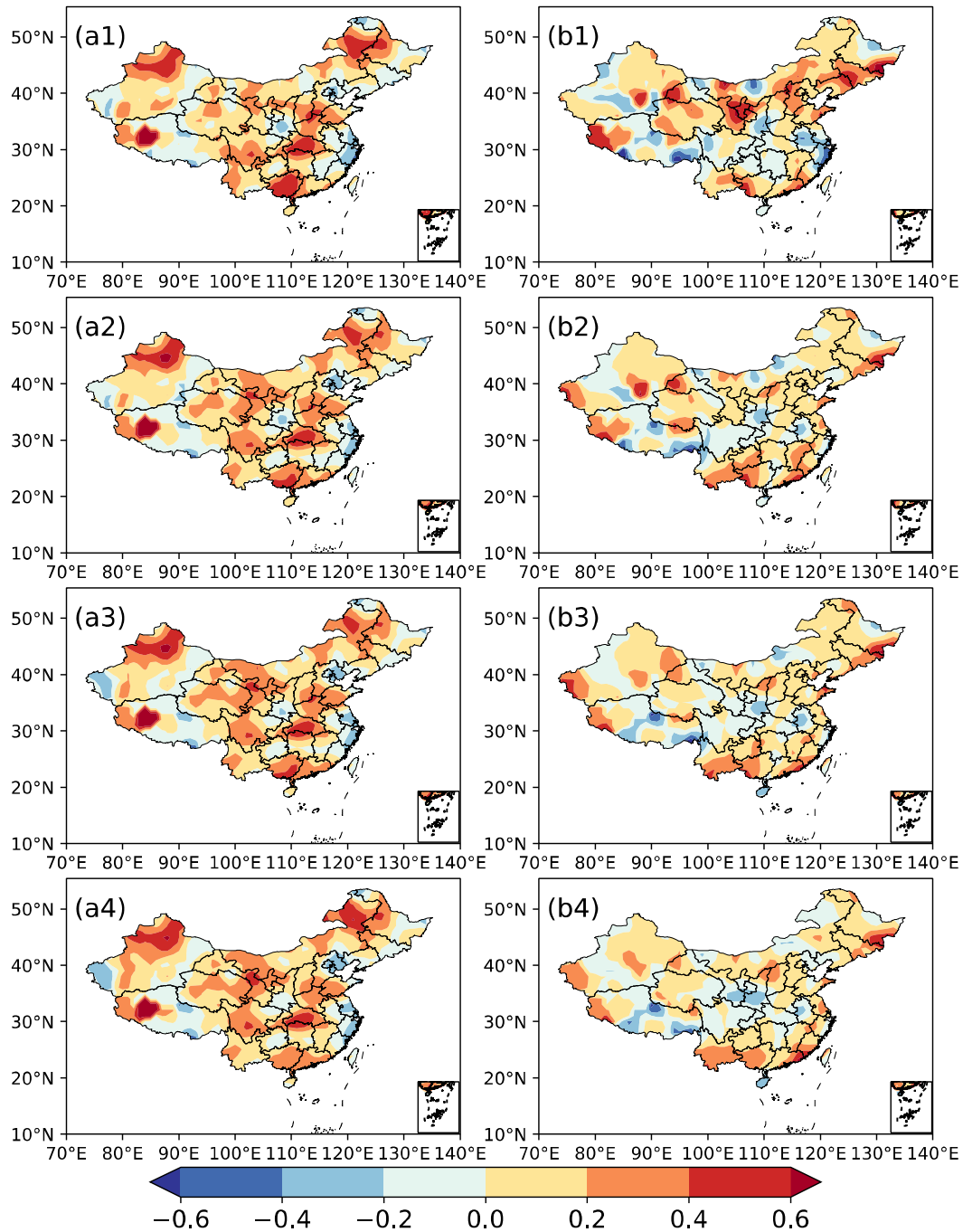
Fig. 4 Spatial distribution of TCC of station-based UWE for summer precipitation in
China during 2011-2020 (a1-a4), TCC differences of station-based ensemble minus

403   the grid-based ensemble (b1-b4). (a1, b1) Ensemble scheme E1; (a2, b3) Ensemble
404   scheme E2; (a3, b3) Ensemble scheme E3; (a4, b4) Ensemble scheme E4.
405
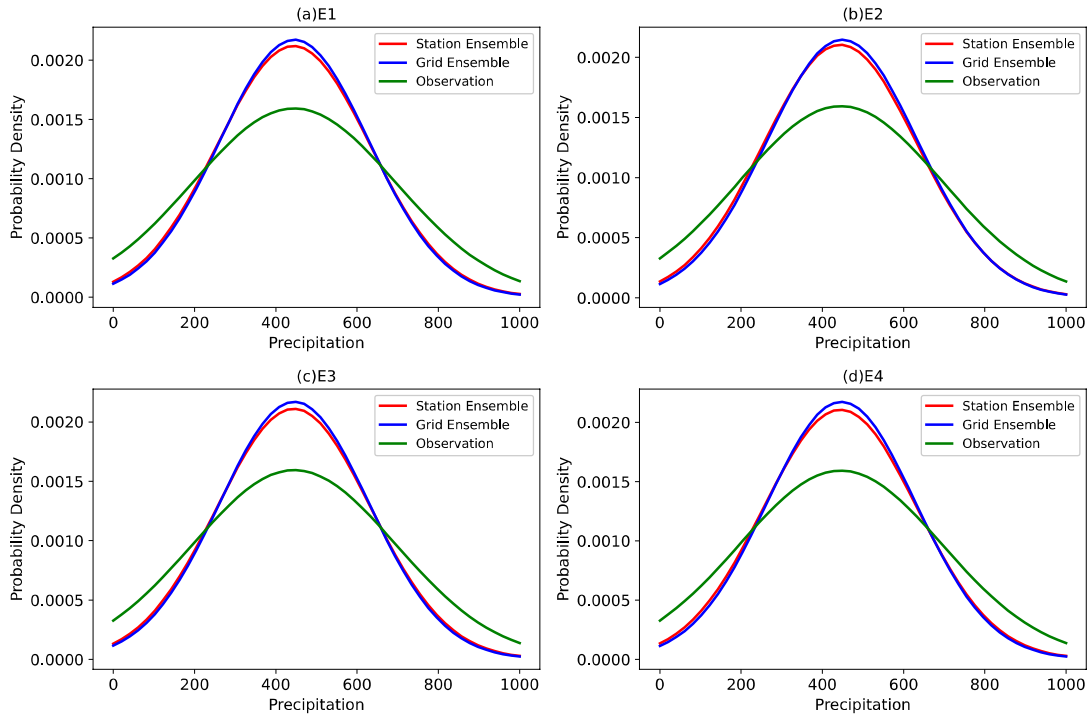
406
407   **Fig. 5** Probability density distribution of the total precipitation for observation and
408   UWE. (a) Ensemble Scheme E1, (b) Ensemble Scheme E2, (a) Ensemble Scheme E3,
409   (a) Ensemble Scheme E4.
410

3 Calculating the spatial similarity of ensemble prediction.

In Fig. 6, the SACCs and RACCs are not consistent with each other, and the former are more frequently lower than the latter. The 10-year average values of SACC for each ensemble prediction for summer precipitation in China are also lower than the RACC (table 1). The SACC is calculated after subtracting the spatial average of anomaly for all the stations from the original precipitation anomaly. This approach may cause the new value for each station can't reflect the real situation and lead to a decrease of RACC between the prediction and observation. In fig.7 the correlation between the RACC and PS are all higher than those between the SAAC and PS, which further indicated RACC can better assess the prediction skill of summer precipitation. It is also noted that the differences between the SACC and RACC are quite obvious in 2011 and 2015 for ensemble schemes E2, E3, and E4 (Fig. 6 b, c, d). Comparing with the PS scores, it seems that the RACC for each prediction have more consistent feature than the SACC.

424 In order to figure out if the RACC has the better performance than the SACC on
425 indicating the spatial consistency of precipitation prediction, the observation and
426 prediction of summer precipitation in 2011 and 2015 are respectively presented in Fig.
427 7. Comparing with the observation (Fig. 7 a5), predicted precipitation anomalies in
428 summer 2011 show consistent feature in most China (Fig. 7 a1-a4). The PS scores of
429 four ensemble schemes are respectively 69.5, 68.7, 73.5, 74.3, and RACCs are 0.08,
430 0.07, 0.10, 0.11, which properly indicate the prediction skill of these four predictions
431 on the summer precipitation in 2011. It is also noted that the SACCs of 2011 prediction
432 are respectively 0.01, -0.08, -0.11 and -0.14, which obviously have flaws in assessing
433 the performance of these four schemes on predicting the precipitation. This
434 shortcoming of the SACC is also exhibited in the prediction of summer precipitation
435 anomalies in 2015 (Fig. 7 b1-b5), owing to its improperly low SACC values being 0.01,
436 -0.07, -0.13, -0.17, respectively.

437

438 **Table 3** 10-year average of RACC, SACC of station-based ensemble predictions for
439 summer precipitation in China during 2011-2020.

	E1	E2	E3	E4
RACC	0.11	0.11	0.11	0.10
SACC	0.10	0.08	0.07	0.05

440

441
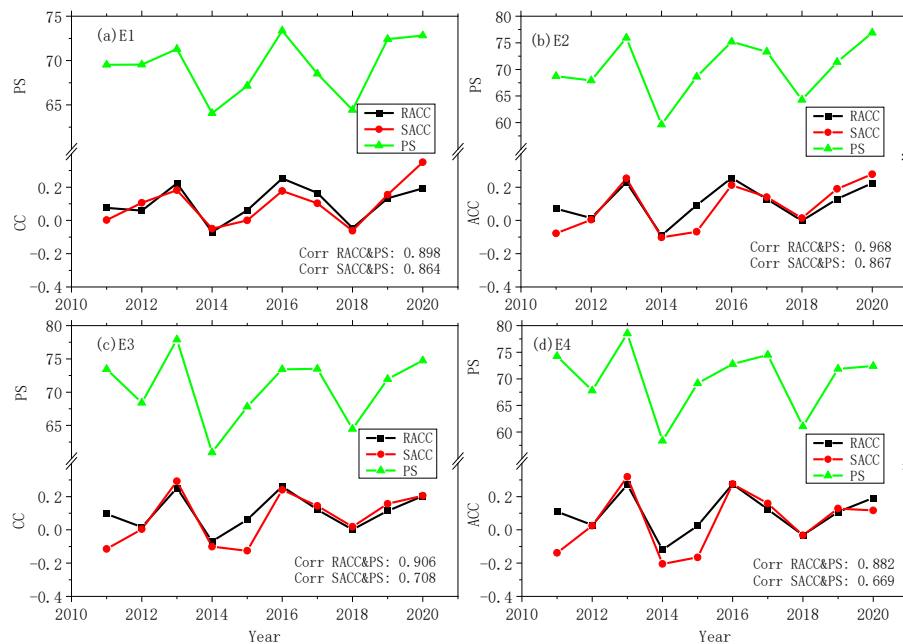
442 **Fig. 6** Annual **R**ACC, SACC and PS of station-based ensemble predictions for

445
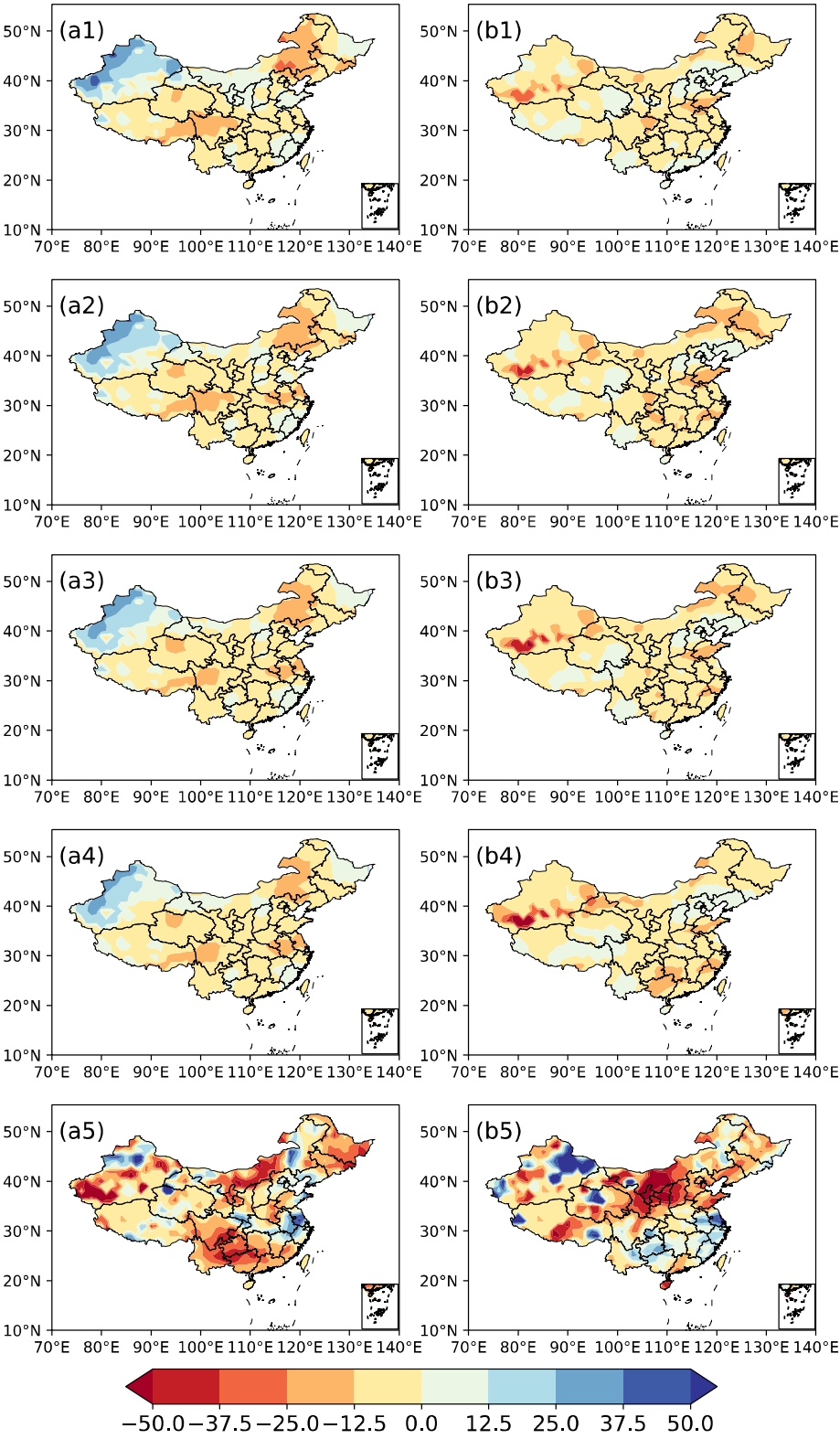
Fig. 7 The spatial distribution of anomalies (unit: %) of observation and prediction of

summer precipitation in 2011 and 2015. (a1-a4) prediction of scheme E1-E4, and (a5)

448   observation for 2011; (b1-b4) prediction of scheme E1-E4, and (b5) observation for

449   2015.

450

451   **4. Impact of dispersal intensity on the ensemble prediction.**

452   The dispersal intensity (Di) also called as the coefficient of variation, which is a

453   variable measure the differences among single samples and can be calculated by formal

454   (8). The dispersal intensity is also a relative measure of variability that indicates the

455   size of a standard deviation in relation to its mean. It is a standardized, unitless measure

456   that allows you to compare variability between disparate groups and

457   characteristics (Tyralis and Papacharalampous 2024).

458
$$Di = \frac{\sqrt{\sum_{k=1}^{n}(F_{km}-\overline{F}_m)^2/n}}{\overline{F}_m} \tag{8}$$

459   Since the dispersal intensity of each statistic-dynamic prediction has obvious

460   interannual variation, it is necessary to analyze its probable impact on the ensemble

461   prediction of summer prediction in China. Fig. 8 presents the relationship of ACC -

462   dispersal intensity of summer precipitation prediction, in which high ACCs of summer

463   precipitation prediction mostly corresponds to the low dispersal intensity among

464   statistic-dynamic predictions. The variabilities of the signal and noise for the ensemble

465   prediction can be measured as the variance of the ensemble mean and ensemble spread

466   of all the initial conditions (Zheng, Wang et al. 2009, Liu, Tang et al. 2019), the

467   sampling error on measuring the signal variance, the more reasonable estimation of the

468   signal variance can be given and used to measure the overall potential predictability of

469   the prediction system (DelSole 2004, DelSole and Tippett 2007). The UWE has the

470   similar theory as the ensemble prediction, the low dispersal intensity among ensemble

471   samples implies the historical similar error selected by different approach is quite close

472   to each other, which makes the correction on the model prediction is more trustable and

473   then produce a more accurate prediction than those cases with high dispersal intensity.

474
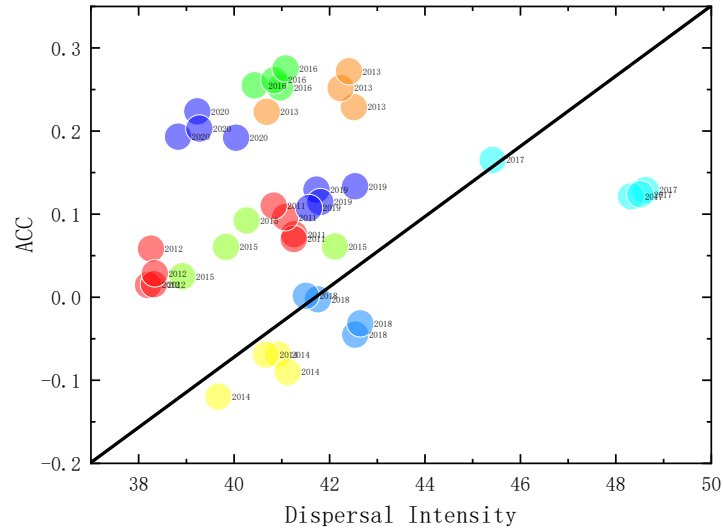
475   **Fig. 8** The relationship between each UME's ACC and the dispersal intensity of each

476   summer precipitation prediction during 2011-2020. The four dots of each color

477   indicate the four schemes (E1-E4) applied in ear year's dynamic-statistic prediction.

478

479

480
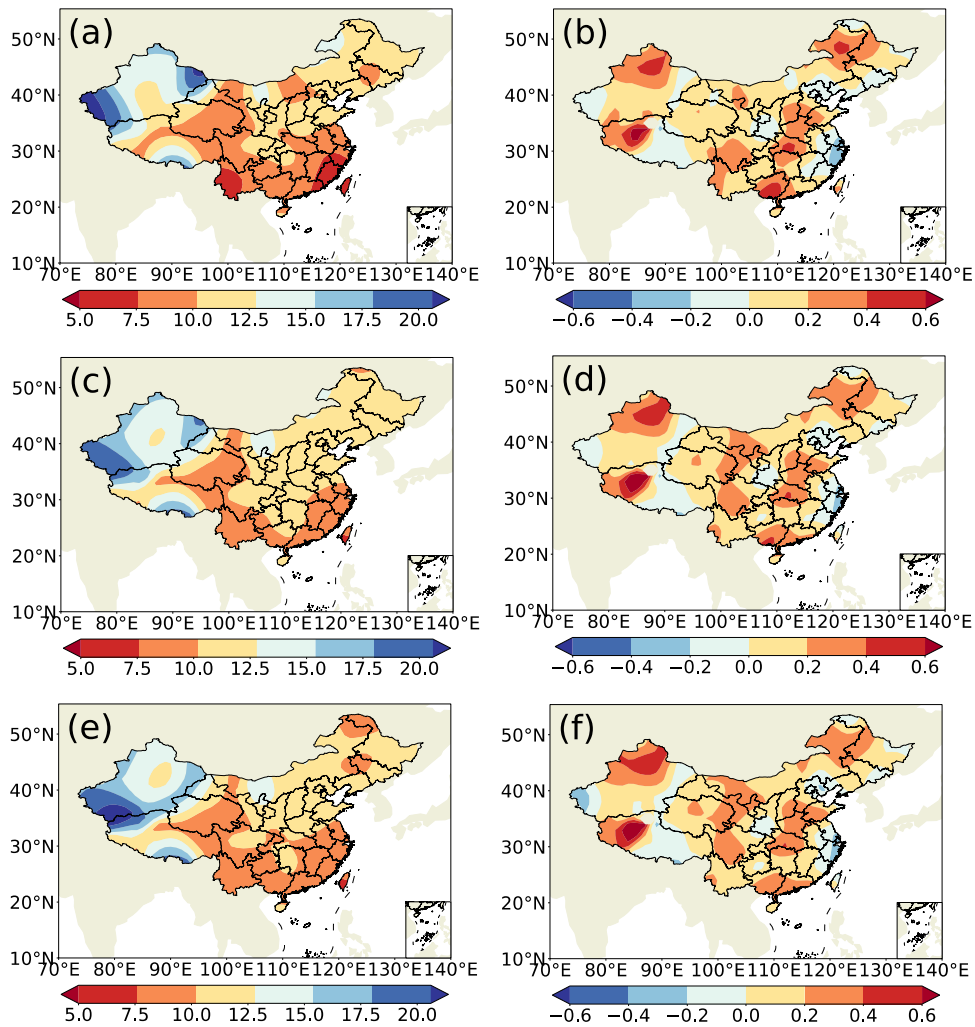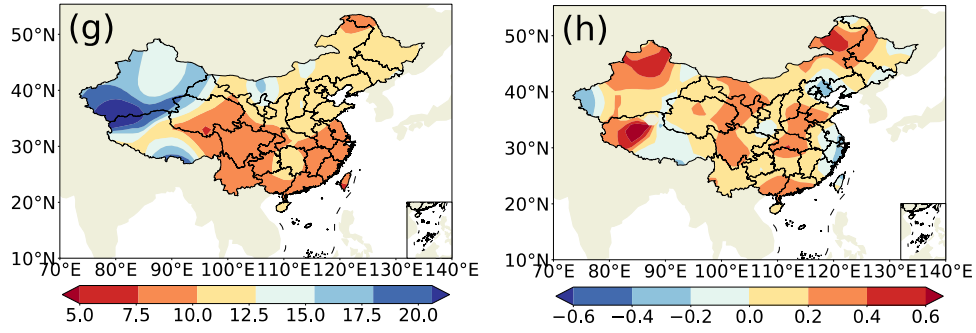
Fig. 9 The spatial distinction of the 10-year average of dispersal intensity (a, c, e, g) and TCC (b, d, f, h) of UME scheme of E1-E4 during 2011-2020.

In Fig. 9, the 10-year average of dispersal intensity of each UME scheme show the similar pattern as the spatial distribution of TCC of summer prediction produced by UME. Except for part of Northwest China and middle East China, the low dispersal intensity also tends to produce high TCC of statistic-dynamic combined ensemble prediction in most China. In the middle region of China, the negative correlation between the dispersal intensity and TCC is not so evident. This could be due to the limitations of the parameterization schemes in the forecast models for this region, which may result in inaccurate simulations of the diffusion process. Additionally, the diversity of meteorological conditions in the middle region could lead to inconsistencies in the relationship between dispersal intensity and TCC across different areas. For instance, the middle region may be influenced by specific meteorological systems, such as frontal systems and cyclones, which can affect the relationship between dispersal intensity and TCC. Therefore, the positive relationship between the dispersal intensity and the ACC can be found in this study, however this kind of relationship has uncertainty in different areas, which still need to be considered in the operational predictions. These aspects require further detailed investigation. In conclusion, The low dispersal intensity among the single prediction corresponds to the major physical process captured by each prediction scheme is similar with each other, which is help of the more reasonable estimation of the signal variance and produce the better precipitation predictions.

5. Conclusions and discussion

This study presents the UWE of the dynamic-statistic schemes in order to enhance summer precipitation prediction in China. The analysis also includes an examination of factors that may impact the prediction skill of UWE, such as grid-based and station-

509 based prediction, the calculation of prediction skill, and the influence of sample
510 dispersion on prediction accuracy.

511   UWE's performance surpasses the model and the dynamic-statistic scheme
512 predictions, potentially due to its ability to overcome individual model or scheme
513 inadequacies, reduce formulation uncertainties, and yield a more stable and accurate
514 predictions. The average RACC and PS values for the five dynamic-statistic schemes
515 that were ensemble members are 0.02-0.10 and 67.4-69.6. In contrast, the grid-based
516 ensemble prediction of UWE becomes 0.04-0.09 and 69.2-70.9, which is an
517 improvement compared to the dynamic-statistic schemes. Station-based ensemble
518 prediction shows superior performance for this well compared to grid-based ensemble
519 prediction and dynamic-statistic methods, achieving average RACC values of 0.10-0.11
520 and PS values of 69.3-70.7.

521   The average RACC and PS values for the station-based ensemble prediction
522 fluctuated between 0.10-0.11 and 69.3-70.2 from 2011 to 2020, indicating significantly
523 higher proficiency compared to the grid-based ensemble prediction. The ensemble
524 prediction based on station data can produce precipitation with a probability density
525 distribution function that is closer to the observed data compared to the grid-based
526 prediction, making the former more accurate. The use of the SACC needs to remove
527 the spatial average of the whole stations from the original value, which may produce
528 inaccurate station values and lead to a lower correlation between predictions and
529 observations. This makes SACC unsuitable for estimating the spatial consistency of
530 summer precipitation predictions. The commonly used SACC should be supplanted by
531 the updated RACC, which is computed by directly utilizing the precipitation anomalies
532 at each station, without the need to deduct the overall average precipitation anomaly
533 from all stations.

534   Moreover, the higher RACCs in summer precipitation prediction are
535 predominantly associated with lower dispersal intensity among the dynamic-statistic
536 predictions. This indicates that a more concentrated ensemble, where predictions are
537 closely aligned, tends to result in more accurate forecasts. Accordingly, the dispersal
538 intensity of ensemble samples is a crucial factor affecting the prediction accuracy of
539 dynamic-statistic combined UWE. UWE shares a similar theoretical foundation with
540 ensemble prediction. Low dispersal intensity among ensemble samples suggests that
541 the historical similar errors identified by various methods are closely aligned. This
542 alignment enhances the reliability of corrections applied to model predictions, thereby

543 yielding more accurate forecasts compared to cases with high dispersal intensities.

544

545 **Acknowledgement,** This work is supported by the National Natural Science Foundation of China
546 Project (Nos.42130610, 42075057, and 42275050) and the National Key Research and Development
547 Program of China (2022YFE0136000). The Sixteenth Graduate Student Research and Innovation
548 Program of Yunnan University (KC-242410028).

549

550 **Author contributions.** The conception of this paper is supposed by Xiaojuan Wang and Guolin.
551 Material preparation, data collection, and analysis were performed by Xiaojuan Wang and Zihan Yang.
552 The manuscript is written by Xiaojuan Wang and revised by Qingquan Li. All authors commented on
553 previous versions of the manuscript. All the authors have read and approved the final manuscript.

554

555 **Funding**. The National Natural Science Foundation of China Project (Nos. 42130610, 42075057, and
556 42275050), The National Key Research and Development Program of China (2022YFE0136000). The
557 Sixteenth Graduate Student Research and Innovation Program of Yunnan University (KC-242410028).

558 **Data Availability Statement**. The datasets generated during and/or analyzed during the current study
559 are available from the corresponding author on reasonable request.

560 **Ethics declarations.** The authors declare no conflict of interest. Authors have no additional information
561 that might be relevant for the editors, reviewers and readers. The funding sponsors have no participation
562 in the execution of the experiment, the decision to publish the results, nor the writing of the manuscript.

563

564 **Conflict of interest:** The authors have no relevant financial or non-financial interests to disclose.

565

566 **Reference**

567 Bueh, C., et al. (2008). "Features of the EAP events on the medium-range evolution

568 process and the mid- and high-latitude Rossby wave activities during the Meiyu

569 period." Chinese Science Bulletin **53**(4): 610-623.

570

571 Candille, G. (2009). "The multiensemble approach: The NAEFS example." Mon.

572 Weather Rev. **137**: 1655–1665.

573

574 Chou, J. (1974). "A problem of using past data in numerical weather forecasting

575 (in Chinese)." **6**: 635-644

576

577 DelSole, T. (2004). "Predictability and information theory. Part I: measures of

578 predictability." J Atmos Sci **61**: 2425–2440.

579

580 DelSole, T. and M. K. Tippett (2007). "Predictability: recent insights from

581 information theory." Rev. Geophys. **45**: 4002.

582

583 Ding, R. and K. H. Seo (2010). "Predictability of the Madden-Julian Oscillation

584 Estimated Using Observational Data." Monthly Weather Review **138**(3): 1004-

585 1013.

586

587 Ding, Y. (1994). "Monsoons over China. Advances in Atmospheric Sciences."

588 Advances in Atmospheric Sciences **11**: 252.

589

590 Ding, Y., et al. (2004). "Advance in Seasonal Dynamical Prediction Operation in

591 China." Acta Meteorologica Sinica **30**(5): 598-612.

592

593 Fan, K., et al. (2012). "Improving the Prediction of the East Asian Summer Monsoon:

594 New Approaches." Weather and Forecasting **27**(4): 1017-1030.

595

596   Feng, G., et al. (2020). "Improved prediction model for flood-season rainfall based

597   on a nonlinear dynamics-statistic combined method." Chaos, Solitons & Fractals

598   **140**: 110160.

599

600   Feng, G., et al. (2013). "Recent progress on the objective and quantifiable forecast

601   of summer precipitation based on dynamical statistical method." J. Appl. Meteor.

602   Sci **24**: 656-665.

603

604   Gettelman, A., et al. (2022). "The future of Earth system prediction: Advances in

605   model-data fusion." SCIENCE ADVANCES **8**: eabn3488.

606

607   Gong, Z., et al. (2017). "Limitations of BCC_CSM's ability to predict summer

608   precipitation over East Asia and the Northwestern Pacific." Atmospheric Research

609   **193**: 184-191.

610

611   Gong, Z., et al. (2016). "Methods for Improving the Prediction Skill of Summer

612   Precipitation over East Asia–West Pacific." Weather and Forecasting **31**(4): 1381-

613   1392.

614

615   Gong, Z., et al. (2018). "Assessment and Correction of BCC_CSM's Performance in

616   Capturing Leading Modes of Summer Precipitation over North Asia." International

617   Journal of Climatology **38**(5): 2201-2214.

618

619   Houze, R. A., et al. (2015). "The variable nature of convection in the tropics and

620   subtropics: A legacy of 16 years of the Tropical Rainfall Measuring Mission

621   satellite." Rev. Geophys. **53**: 994–1021.

622

623   Huang, G. (2004). "An Index Measuring the Interannual Variation of the East Asian

624   Summer Monsoon—The EAP Index." Adv. Atmos. Sci. **21**(1): 41-52.

625

626   Huang, J., et al. (1993). "An analogue-dynamical long-range numerical weather

627   prediction system incorporating historical evolution." Quarterly Journal of the

628   Royal Meteorological Society **119**(511): 547-565.

629

630   Huang, R. (1987). Influence of the heat source anomaly over the tropical western

631   Pacific on the subtropical high over East Asia. International Conference on the

632   General Circulation of East Asia, Chengdu.

633

634   Kim, H.-M., et al. (2012). "Seasonal prediction skill of ECMWF System 4 and NCEP

635   CFSv2 retrospective forecast for the Northern Hemisphere Winter." Climate

636   Dynamics **39**(12): 2957-2973.

637

638 Krishnamurti, T. N. and V. Kumar (2012). "Improved seasonal precipitation

639 forecasts for the Asian Monsoon using a large suite of atmosphere ocean coupled

640 models: Anomaly." J. Clim. **25**: 65–88.

641

642 Krishnamurti, T. N., et al. (2016). "A review of multimodel superensemble

643 forecasting for weather, seasonal climate, and hurricanes." Reviews of Geophysics

644 **54**(2): 336-377.

645

646 Lang, X. and H. Wang (2010). "Improving Extraseasonal Summer Rainfall

647 Prediction by Merging Information from GCMs and Observations." Weather and

648 Forecasting **25**(4): 1263-1274.

649

650 Li, H., et al. (2008). "Responses of East Asian summer monsoon to historical SST

651 and atmospheric forcing during 1950–2000." Climate Dynamics **34**(4): 501-514.

652

653 Li, J. and R. Ding (2011). "Temporal-Spatial Distribution of Atmospheric

654 Predictability Limit by Local Dynamical Analogs." Monthly Weather Review

655 **139**(10): 3265-3283.

656

657 Li, X., et al. (2020). "Quantitative Comparison of Predictabilities of Warm and Cold

658 Events Using the Backward Nonlinear Local Lyapunov Exponent Method."

659 Advances in Atmospheric Sciences **37**(9): 951-958.

660

661 Li, X., et al. (2020). "Quantitative study of the relative effects of initial condition

662 and model uncertainties on local predictability in a nonlinear dynamical system."

663 Chaos, Solitons & Fractals **139**(1).

664

665 Liu, T., et al. (2019). "The relationship among probabilistic, deterministic and

666 potential skills in predicting the ENSO for the past 161 years." Climate Dynamics

667 **53**(11): 6947-6960.

668

669 Lu, R. Y. (2005). "Interannual variation of North China rainfall in rainy season and

670 SSTs in the equatorial eastern Pacific." Chinese Science Bulletin **50**(18): 2069-2073.

671

672 Luo, L., et al. (2007). "Bayesian merging of multiple climate model forecasts for

673 seasonal hydrological predictions." J. Geophys. Res. Atmos. **112**: D10102.

674

675 Palmer, T. N., et al. (2004). "Development of a European multimodel ensemble

676 system for seasonal-to-interannual prediction (DEMETER)." Bull. Am. Meteorol.

677 Soc. **85**: 853–872.

678

679 Ren, H. L. and J. F. Chou (2006). "Introducing the updating ofmulti reference states

680 into dynamical analogue prediction." ActaMeteor. Sinica **64**: 315–324.

681

682 Ren, H. L. and J. F. Chou (2007). "Strategy and methodology ofdynamical analogue

683 prediction." Sci. China (D) **50**: 1589–1599.

684

685 Roberts, M. J., et al. (2016). "Impact of ocean resolution on coupled air-sea fluxes

686 and large‐scale climate." GEOPHYSICAL RESEARCH LETTERS **43**(19): 10,430-

687 410,438.

688

689 Satoh, M., et al. (2014). "The non-hydrostatic icosahedral atmospheric model:

690 Description and development." Progress in Earth and Planetary Science **1**(1): 1-

691 32.

692

693 Si, D. and Y. Ding (2013). "Decadal change in the correlation pattern between the

694 Tibetan Plateau winter snow and the East Asian summer precipitation during

695 1979–2011." Journal of Climate **26**(19): 7622-7634.

696

697 Specq, D. and L. Batté (2020). "Improving subseasonal precipitation forecasts

698 through a statistical–dynamical approach: application to the southwest tropical

699 Pacific." Clim. Dyn. **55**: 1913–1927.

700

701 Sun, L., et al. (2021). "Changing Impact of ENSO Events on the Following Summer

702 Rainfall in Eastern China since the 1950s." Journal Of Climate **34**(20): 8105-8123.

703

704 Tao, S. (2006). "The Westward,Northward Advance of the Subtropical High over

705 the West Pacific in Summer." Journal of Applied Meteorological Science.

706

707 Tyralis, H. and G. Papacharalampous (2024). "A review of predictive uncertainty

708 estimation with machine learning." Artificial Intelligence Review **57**(4): 94.

709

710 Vitart, F. (2006). "Seasonal forecasting of tropical storm frequency using a multi-

711 model ensemble." Q. J. R. Meteorol. Soc. **132**: 647–666.

712

713 Wang, H. and K. Fan (2009). "A New Scheme for Improving the Seasonal Prediction

714 of Summer Precipitation Anomalies." Weather and Forecasting **24**(2): 548-554.

715

716 Wang, H., et al. (2015). "A review of seasonal climate prediction research in China."

717 Advances in Atmospheric Sciences **32**(2): 149-168.

718

719 Wang, Q. J., et al. (2012). "Merging Seasonal Rainfall Forecasts from Multiple

720 Statistical Models through Bayesian Model Averaging." Journal Of Climate **25**(16):

721 5524-5537.

722

723 Wu, J., et al. (2017). "Simulations of the Asian summer monsoon in the sub-

724 seasonal to seasonal prediction project (S2S) database." Quarterly Journal of the

725 Royal Meteorological Society **143**: 706-727.

726

727   Wu, T., et al. (2021). "BCC-CSM2-HR: A High-Resolution Version 1 of the Beijing

728   Climate Center Climate System Model." Geosintific Model Development **14**: 2977–

729   3006.

730

731   Xiong, K., et al. (2011). "Analogue-dynamical prediction of monsoon precipitation

732   in Northeast China based on dynamic and optimal configuration of multiple

733   predictors." Acta. Meteor. Sin. **25**: 316–326. .

734

735   Xiong, K. G., et al. (2011). "Analogue-dynamical prediction of monsoon

736   precipitation in Northeast China based on dynamic and optimal configuration of

737   multiple predictors." J. Meteor. Sci **25**(3): 316-326.

738

739   Yan, X. and Y. Tang (2013). "An analysis of multi-model ensembles for seasonal

740   climate predictions." Quarterly Journal of the Royal Meteorological Society

741   **139**(674): 1179-1198.

742

743   Yang, J., et al. (2012). "Estimating the Prediction Errors of Dynamical Climate

744   Model on the Basis of Prophase Key Factors in North China." Chin. J. Atmos. Sci.

745   **36**: 11-22.

746

747 Yang, Z., et al. (2024). "Analysis on the station-based and grid- based integration

748 for dynamic-statistic combined predictions." **155**(6): 5184.

749

750 Zheng, F., et al. (2009). "ENSO ensemble prediction: Initial error perturbations vs.

751 model error perturbations." Chinese Science Bulletin **54**(14): 2516-2523.

752

753 Zhu, J. and J. Shukla (2013). "The role of air–sea coupling in seasonal prediction

754 of Asia–Pacific summer monsoon rainfall." Journal of Climate **26**(15): 5689-5697.

755
756
757